Effect of external mechanical constraints on the phase diagram of epitaxial $PbZr_{1-x}Ti_xO_3$ thin films—thermodynamic calculations and phase-field simulations

Y. L. Li,[a] S. Choudhury, Z. K. Liu, and L. Q. Chen
Department of Materials Science and Engineering, The Pennsylvania State University, University Park, Pennsylvania 16802

(Received 17 February 2003; accepted 13 June 2003)

The phase diagram of a $PbZr_{1-x}Ti_xO_3$ (PZT) film constrained by a much thicker substrate was studied using both thermodynamic calculations and phase-field approach. It was found that the ferroelectric transition temperature is increased with substrate constraint regardless of the nature of the constraint, i.e., tensile or compressive. The maximum increase in the transition temperature occurs near $x=0.5$, and the morphotropic phase boundary is shifted considerably by the substrate constraint. It is shown that the orthorhombic phase ($|P_1|=|P_2|\neq 0$, $P_3=0$) that does not exist in the bulk becomes stable under a tensile constraint, and the rhombohedral phase ($|P_1|=|P_2|=|P_3|\neq 0$) in the bulk is distorted in the constrained film, i.e., $|P_1|=|P_2|\neq 0$, $|P_3|\neq 0$. The phase diagrams obtained by the phase-field approach indicated that the stability region for the tetragonal phase is much wider than that obtained from the thermodynamic calculations assuming a single-domain, especially under tensile substrate constraint. The discrepancy between the two methods becomes larger as substrate constraint changes from compressive to tensile, implying that thermodynamic calculations are unreliable for constructing stability diagram of PZT, particularly under a tensile constraint. © *2003 American Institute of Physics.* [DOI: 10.1063/1.1600824]

Lead zirconate-titanate [$PbZr_{1-x}Ti_xO_3$ (PZT)] has been extensively studied due to its wide technological applications as piezoelectric transducers, pyroelectric detectors, electro-optic devices, and explosively induced charge storage devices.[1,2] Its bulk phase stability under the stress-free boundary condition is reasonably known[1–7] although recent studies have found additional phases in the system near the morphotropic boundary.[8] During the last few years, there has been an increasing interest in growing epitaxial PZT films to explore their potential applications in nonvolatile memory devices, infrared sensors, and microelectromechanical systems.[9–13] For a PZT film, the phase stability could be drastically modified by a substrate constraint as it has been shown recently for other systems.[14–18] The effect of a constant applied stress on the phase diagram of a film has recently been studied.[19] In this work, we employ both thermodynamic calculations and phase-field approach to investigate the effect of substrate constraint, a biaxial strain, on the phase diagram of a PZT film.

To describe a proper ferroelectric transition, the spontaneous polarization $\mathbf{P}=(P_1,P_2,P_3)$ is chosen as the order parameter. The bulk free energy density as a function of polarization was modeled by Haun *et al.*[2,7] using a six-order polynomial in polarization, i.e.:

$$\begin{aligned} f_{\text{lan}} &= \alpha_1(P_1^2+P_2^2+P_3^2)+\alpha_{11}(P_1^4+P_2^4+P_3^4) \\ &+ \alpha_{12}(P_1^2P_2^2+P_2^2P_3^2+P_3^2P_1^2)+\alpha_{111}(P_1^6+P_2^6+P_3^6) \\ &+ \alpha_{112}[P_1^2(P_2^4+P_3^4)+P_2^2(P_1^4+P_3^4)+P_3^2(P_1^4+P_2^4)] \\ &+ \alpha_{123}P_1^2P_2^2P_3^2, \end{aligned} \tag{1}$$

where α_1, α_{11}, α_{12}, α_{111}, α_{112}, and α_{123} are the dielectric stiffnesses and higher order stiffness under a stress-free condition, and they are functions of composition.[7] For the sake of simplification, the antiferroelectric transition and the rotation of oxygen octahedron, which might occur at low temperatures when x is close to zero, are ignored, since we are mostly interested in the shift of the transition temperature of paraelectric to ferroelectric as well as the shift of the morphotropic phase boundary under a substrate constraint.

The elastic energy density at a given strain state is given by

$$\begin{aligned} f_{\text{ela}} &= \tfrac{1}{2}c_{ijkl}e_{ij}e_{kl}=\tfrac{1}{2}c_{ijkl}(\varepsilon_{ij}-\varepsilon_{ij}^0)(\varepsilon_{kl}-\varepsilon_{kl}^0), \\ &= \tfrac{1}{2}c_{ijkl}(\varepsilon_{ij}-Q_{ijmn}P_mP_n)(\varepsilon_{kl}-Q_{klmn}P_mP_n), \\ &= \tfrac{1}{2}c_{ijkl}Q_{ijmn}Q_{klst}P_mP_nP_sP_t-c_{ijkl}\varepsilon_{ij}Q_{klmn}P_mP_n \\ &+ \tfrac{1}{2}c_{ijkl}\varepsilon_{ij}\varepsilon_{kl}, \end{aligned} \tag{2}$$

where $e_{ij}=\varepsilon_{ij}-\varepsilon_{ij}^0$ is elastic strain, ε_{ij} is the strain state of the crystal compared to the parent paraelectric phase, c_{ijkl} is the elastic stiffness tensor, and ε_{ij}^0 is the stress-free strain or transformation strain or eigenstrain: $\varepsilon_{ij}^0=Q_{ijkl}P_kP_l$, where Q_{ijkl} is the electrostrictive coefficient. Therefore, changing from a stress-free boundary condition to a clamped one modifies the second-order and the fourth-order terms of the Landau free-energy polynomial in Eq. (1), and thus the nature of a ferroelectric transition and its transition temperature.[16,20] Since this work emphasizes the effect of substrate constraint, any surface and interfacial contribution and electrostatic energy are ignored. The effect of electrostatic energy was discussed in our previous letter.[21]

We choose a rectangular coordinate system $\mathbf{x}=(x_1,x_2,x_3)$ with x_3 normal to the film and consider a (001)

[a]Electronic mail: yil1@psu.edu

 © 2003 American Institute of Physics
Downloaded 14 Apr 2007 to 128.118.88.141. Redistribution subject to AIP license or copyright, see http://apl.aip.org/apl/copyright.jsp

PZT film grown on a (001) cubic substrate. We assume that the substrate is much thicker than the film. For the case of a single domain in the film, i.e., the polarization is constant throughout the entire film, and thus the stress and strain fields are homogeneous. With this coordinate system, ε_{11}, ε_{22}, and ε_{12} are the strain components parallel to the film surface and are determined by the substrate constraint, $\varepsilon_{11}=\varepsilon_{22}=e_0$ where e_0 is the strain constraint from the substrate, and $\varepsilon_{12}=\varepsilon_{21}=0$. The other strains ε_{i3} are solved from the mechanical equilibrium equation subject to the stress-free surface condition: $\varepsilon_{33}=\lfloor q_{12}(P_1^2+P_2^2)+q_{11}P_3^2-2c_{12}e_0\rfloor/c_{11}$, $\varepsilon_{13}=\varepsilon_{31}=q_{44}P_1P_3/2c_{44}$, and $\varepsilon_{23}=\varepsilon_{32}=q_{44}P_2P_3/2c_{44}$, where $q_{11}=c_{11}Q_{11}+2c_{12}Q_{12}$, $q_{12}=c_{12}Q_{11}+(c_{11}+c_{12})Q_{12}$, $q_{44}=2c_{44}Q_{44}$. c_{ij} and Q_{ij} are the corresponding elastic stiffness and electrostrictive coefficients for the cubic PZT in Voigt's notation.

The thermodynamically most stable single-domain state is obtained by minimizing the bulk free energy density and the elastic energy density under a given substrate constraint, temperature and composition. We consider three cases, $e_0=-0.005$, 0.0, $+0.005$. The Landau coefficients and the electrostrictive coefficients are taken from the work of Haun *et al.*[2–7] The elsatic stiffness is taken as constant for all x as: $c_{11}=1.796\times10^{11}$, $c_{12}=7.937\times10^{10}$, $c_{44}=1.111\times10^{11}$ (Nm^{-2}). The corresponding phase diagrams assuming a single-domain state are shown using solid lines in Figs. 1–3. The bulk phase diagram under stress-free is given in Fig. 2 in dashed lines for comparison, which shows that under stress-free there are two stable ferroelectric phases, i.e., tetragonal ($P_1\neq0$, $P_2=P_3=0$, or $P_2\neq0$, $P_1=P_3=0$, or $P_3\neq0$, $P_1=P_2=0$) and rhombohedral ($|P_1|=|P_2|=|P_3|\neq0$) depending on the mole fraction of $PbTiO_3$ and temperature. Comparing Figs. 1–3 it is shown that the substrate constraint significantly shifted the morphotropic phase boundary and increased the transition temperature. Moreover, the rhombohedral phase ($|P_1|=|P_2|=|P_3|\neq0$) is distorted under a substrate constraint, resulting in $|P_1|=|P_2|\neq0$, $|P_3|\neq0$ which the monoclinic phase possess.[8,16,22] For the case of $e_0=0.005$, the orthorhombic phase ($|P_1|=|P_2|\neq0, P_3=0$), which does not exist in the bulk, becomes a stable ferroelectric phase. It is interesting to notice that the transition temperature is unusually high near $x=0.50$ due to the fact that the electrostrictive coefficients Q_{ij} as function of composition exhibit peaks around $x=0.50$ and the shift in the transition temperature due to substrate constraint is directly proportional to $Q_{11}+Q_{12}$ or Q_{12}.

To incorporate the possibility of multidomain and/or multiphase states in the phase diagram, we employed the phase-field approach by assuming that the polarization field as well as the local strain is inhomogeneous. The inhomogeneous local strain is obtained from the mechanical equilibrium equation, $\partial\sigma_{ij}/\partial x_j=0$, together with the corresponding boundary condition.[20]

For determining the stability of a domain structure, the contribution of the domain wall energy should be considered. It can be introduced through the gradients of the polarization field.[20] The total free-energy as a functional of polarization is

$$F=\int_V f\,dV=\int_V (f_{\mathrm{lan}}+f_{\mathrm{ela}}+f_{\mathrm{gra}})dV. \tag{3}$$

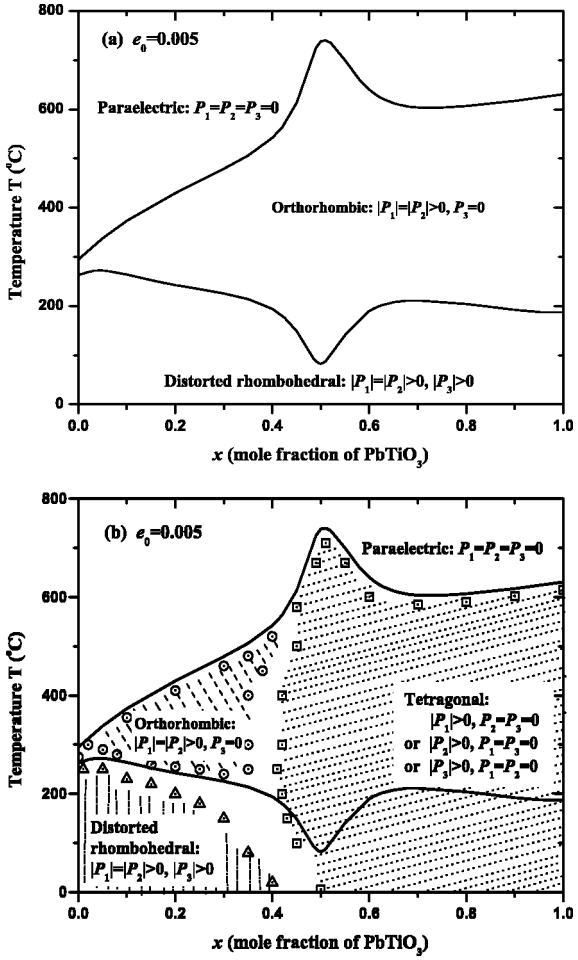

FIG. 1. (a) Phase diagram of PZT film under substrate constraint $e_0=0.005$ obtained using thermodynamic calculations assuming a single-domain state. There are only two stable ferroelectric phases. The solid lines represent the boundaries separating the stability fields of the paraelectric and ferroelectric phases, or the ferroelectric orthorhombic and distorted rhombohedral phases. (b) Superposition of the phase diagram from the phase-field approach (scattered symbols) and from thermodynamic calculations assuming a single-domain assumption [solid lines, same as in (a)]. There are three stable ferroelectric phases (tetragonal—"square," orthorhombic—"circle," and distorted rhombohedral—"triangle") according to the phase-field simulations. The scattered symbols simply represent the ferroelectric domain state obtained at the end of a phase-field simulation. The shaded portion surrounded by the scattered symbols label the stability regions of a single ferroelectric phase, and the nonshaded region shows a mixture of two or three ferroelectric phases.

The temporal evolution of the polarization field from nonequilibrium to equilibrium is described by the time-dependent Ginzburg–Landau equation:

$$\frac{\partial P_i(\mathbf{x},t)}{\partial t}=-L\frac{\delta F}{\delta P_i(\mathbf{x},t)}, \tag{4}$$

where L is a kinetic coefficient which is related to the domain movement.

By solving Eq. (4) numerically using the semi-implicit Fourier-spectral method[23] with periodic boundary conditions along x_1 and x_2 directions, the domain stability maps are obtained for the same three cases $e_0=-0.005, 0.0, +0.005$. For comparison with the results from the thermodynamic calculations assuming a single-domain state, the results are also shown in Figs. 1–3 by the scattered symbols. In these figures, the triangles, circles, and squares represent the pure

Downloaded 14 Apr 2007 to 128.118.88.141. Redistribution subject to AIP license or copyright, see http://apl.aip.org/apl/copyright.jsp

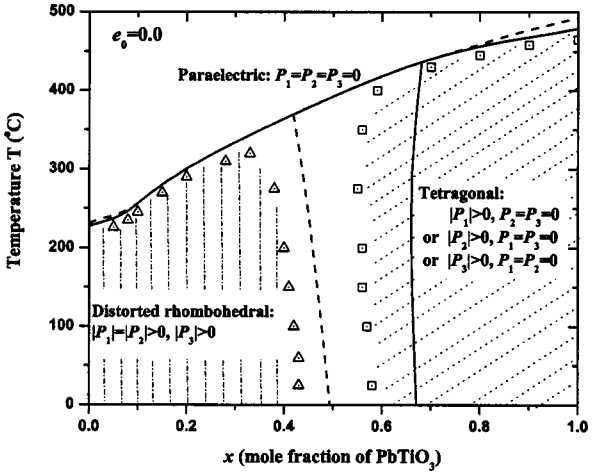

FIG. 2. Comparison of the phase diagrams of a PZT film under the substrate constraint of $e_0=0.0$ obtained from the phase-field approach (scattered symbols) and from thermodynamic calculations assuming a single-domain state (solid lines). The dashed lines are for PZT bulk under stress-free.

distorted-rhombohedral, orthorhombic, and tetragonal phases, respectively, that exist at the end of a simulation by starting from an initial paraelectric state with small random perturbations. The shaded portion indicates the single-phase stability region obtained from phase-field approach while the nonshaded region representing a mixture of two or three ferroelectric phases. Phase field approach shows that tetragonal phase exists as a stable ferroelectric phase at a high mole fraction x of $PbTiO_3$ for all three types of substrate constraints whereas an orthorhombic phase is stabilized at low mole fraction x of $PbTiO_3$ under a tensile substrate constraint. Based on the results (Fig. 1), it is demonstrated that under the tensile substrate constraint the phase diagram calculated assuming a single-domain state and that from the phase-field approach have significant differences. Under the assumption of a single-domain state, there are only two possible stable phases, i.e., orthorhombic and distorted rhombohedral. While from the phase-field simulation, it is found that when the mole fraction $x>0.5$, the tetragonal phase is more stable than orthorhombic or distorted rhombohedral phases. In addition, from the phase-field simulation, there exist regions in the diagram where two or three phases coexist. For the other two cases of $e_0=0.0$ and $e_0=-0.005$, although our phase-field simulations show only two types of stable phases, i.e., tetragonal and distorted rhombohedral, similar to the results from thermodynamic calculations assuming a single-domain state, the position of the morphotropic boundary is different.

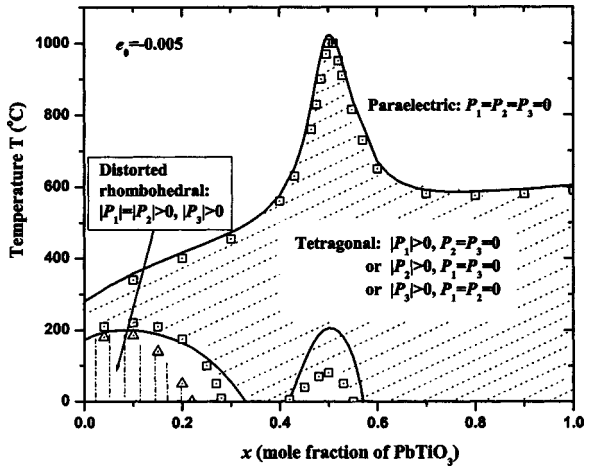

FIG. 3. Comparison of the phase diagrams of a PZT film under the substrate constraint of $e_0=-0.005$ obtained from the phase-field approach (scattered symbols) and from a single-domain assumption (solid lines).

In summary, the phase diagram of PZT film constrained by substrate has been constructed with the phase-field approach for a few representative substrate constraints. It is found that the phase diagram for the PZT film constrained by a substrate is drastically different from the corresponding bulk stress-free phase diagram with different transition temperatures, stable ferroelectric phases, and the position of the morphotropic phase boundary. Our results also demonstrate thermodynamic calculations assuming a single-domain state may result in incorrect stability diagrams.

The financial support from the NSF under DMR-0103354, DMR-0122638, and DMR-9983532 are gratefully acknowledged. The authors would like to acknowledge that the idea to calculate the effect of substrate constraint on the PZT phase diagram was first suggested by Dr. Stephen Streiffer at the Pan American Advances Studies Institute ''Science and Technology of Ferroelectric Materials,'' Rosario Argentina, 23 September–2 October 2002. One of the authors (L.Q.C.) also appreciates useful discussions on the stress effect on domain stabilities with Professor L. E. Cross at the Institute.

[1] B. Jaffe, W. J. Cook, and H. Jaffe, *Piezoelectric Ceramics* (Academic, London, 1971).
[2] M. J. Haun, E. Furman, S. J. Jang, and L. E. Cross, Ferroelectrics **99**, 13 (1989).
[3] M. J. Haun, E. Furman, H. A. McKinstry, and L. E. Cross, Ferroelectrics **99**, 27 (1989).
[4] M. J. Haun, Z. Q. Zhuang, E. Furman, S. J. Jang, and L. E. Cross, Ferroelectrics **99**, 45 (1989).
[5] M. J. Haun, E. Furman, T. R. Halemane, and L. E. Cross, Ferroelectrics **99**, 55 (1989).
[6] M. J. Haun, E. Furman, S. J. Jang, and L. E. Cross, Ferroelectrics **99**, 63 (1989).
[7] M. J. Haun, Thesis, The Pennsylvania State University, 1988.
[8] B. Noheda, D. E. Cox, G. Shirane, J. A. Gonzalo, L. E. Cross, and S. E. Park, Appl. Phys. Lett. **74**, 2059 (1999).
[9] O. Auciello, J. F. Scott, and R. Ramesh, Phys. Today **51**, 22 (1998).
[10] R. Ramesh, S. Aggarwal, and O. Auciello, Mater. Sci. Eng., R. **32**, 191 (2001).
[11] S. P. Alpay, V. Nagarajan, L. A. Bendersky, M. D. Vaudin, S. Aggarwal, R. Ramesh, and A. L. Roytburd, J. Appl. Phys. **85**, 3271 (1999).
[12] J. G. Hong, H. W. Song, S. B. Hong, H. Shin, and K. No, J. Appl. Phys. **92**, 7434 (2002).
[13] Y. Wang, C. Ganpule, B. T. Liu, H. Li, K. Mori, B. Hill, M. Wuttig, R. Ramesh, J. Finder, Z. Yu, R. Droopad, and K. Eisenbeiser, Appl. Phys. Lett. **80**, 97 (2002).
[14] J. S. Speck and W. Pompe, J. Appl. Phys. **76**, 466 (1994).
[15] S. P. Alpay and A. L. Roytburd, J. Appl. Phys. **83**, 4714 (1998).
[16] N. A. Pertsev, A. G. Zembilgotov, and A. K. Tagantsev, Phys. Rev. Lett. **80**, 1988 (1998).
[17] V. G. Koukhar, N. A. Pertsev, and R. Waser, Phys. Rev. B **64**, 214103 (2001).
[18] Y. L. Li, S. Y. Hu, Z. K. Liu, and L. Q. Chen, Appl. Phys. Lett. **78**, 3878 (2001).
[19] S. H. Oh and H. M. Jang, Phys. Rev. B **62**, 14757 (2000).
[20] Y. L. Li, S. Y. Hu, Z. K. Liu, and L. Q. Chen, Acta Mater. **50**, 395 (2002).
[21] Y. L. Li, S. Y. Hu, Z. K. Liu, and L. Q. Chen, Appl. Phys. Lett. **81**, 427 (2002).
[22] Z. G. Ban and S. P. Alpay, J. Appl. Phys. **93**, 504 (2003).
[23] L. Q. Chen and J. Shen, Comput. Phys. Commun. **108**, 147 (1998).

Downloaded 14 Apr 2007 to 128.118.88.141. Redistribution subject to AIP license or copyright, see http://apl.aip.org/apl/copyright.jsp